Analytical Modeling of Line-Tunneling TFETs Based on Low-Bandgap Semiconductors

Bahareh Safari[1], Seyed Ebrahim Hosseini[2*]

[1] Electrical Engineering Department, North Khorasan Science and Research Branch, Bojnourd 94176-97796, Iran
[2] Electrical Engineering Department, Ferdowsi University of Mashhad, Mashhad 9177948944, Iran

Corresponding Author Email: ehosseini@um.ac.ir

ABSTRACT

The combination of two techniques: low-bandgap semiconductor and line-tunneling structure is an effective way to achieve the highest on-current in TFETs. In this paper, design of low-bandgap line-tunneling TEFT and its analytical modeling of drain current equation is proposed. The previously suggested drain current equation for the low-bandgap line-tunneling TEFT has been explained in a relatively complex form based on the minimum tunnel path that is an effective factor in determining band-to-band tunneling (BTBT). It has been simplified in this paper and reformulated based on gate-to-source voltage. Important design factors such as source doping concentration, material and thickness of the gate-insulator were examined by simulation and numerical calculations based on the minimum tunnel path for two low-bandgap $In_{0.88}Ga_{0.12}As$ and relatively high-bandgap GaSb semiconductors. The comparison of the results obtained from simulations with the proposed analytical drain current model show a good agreement. Drain doping concentration, is an effective factor on the off-state current of low-bandgap TFET. This factor was examined in order to reduce the off-current.

1. INTRODUCTION

Nowadays, the down-scaling of conventional MOSFET has led to increase in power consumption [1-4] that has been called as the power crisis [1, 3]. The mechanism of MOSFET transistors operation does not allow subthreshold swing less than 60 mV/dec [5-7]. Tunnel field-effect transistor (TFET) is defined as a semiconductor device in which the gate controls the source-drain current through modulation of Band-to-Band Tunneling (BTBT) and Band-to-Band Tunneling is a process in which electrons tunnel from the valence band through the semiconductor bandgap to the conduction band [8]. The TFET is suitable for low power consumption applications because of its low subthreshold swing and low off-state leakage current. [9-13]. However, Si-based TFETs have a low on-current due to their high-bandgap [14-16]. It has been proved that using low-bandgap semiconductors increases the on-current (I_{on}) of TFET [17-20] although the low-bandgap in these semiconductors, reduces the undesirable tunnel length at the channel-drain side and increases significantly the off-current (I_{off}) [16]. Reducing the drain doping concentration has an important role in decreasing the tunneling of the drain side and controlling the off-current [16]. In the low-bandgap TFET the effect of drain-source voltage (V_{ds}) controlling is more due to its low-bandgap. When (V_{ds}) goes beyond the bandgap voltage (E_g/q), the undesirable tunnel length is significantly decreased. Using gate-source overlap structure or line-tunneling structure is another effective way to increase the on-current in TFETs [1, 8, 21]. Combining the line-tunneling structure and the low-bandgap semiconductor is an effective way to achieve the highest on-current in TEFT [22]. The tunnel path is defined as the physical path between two points corresponding to equal energy for the conduction and valence band respectively [8].

Since the minimum tunnel path (l_{min}) which is the minimum length of tunnel path in the depletion region, has a great effect in determining the amount of the line-tunneling TFET current, important parameters of design such as: source doping concentration, material and the thickness of gate-insulator were investigated by simulation and numerical calculations based on the minimum tunnel path (l_{min}) for two semiconductors, low-bandgap $In_{0.88}Ga_{0.12}As$ and relatively high-bandgap GaSb. The previously proposed current equation for low-bandgap line-tunneling TEFT [22] based on l_{min} is relatively complex. It has been simplified in this paper and it has also been reformulated based on the gate-to-source voltage (V_{gs}). Then, a comparison has been made between the results obtained from the proposed model and the results obtained from the previous model [22] and the simulation results for several different source doping concentrations, gate-insulator with different materials and thicknesses, which showed a good agreement.

2. LOW-BANDGAP LINE-TUNNELING TFET

2.1 Structure and parameters

Figure 1 shows a schematic sketch of the line- and point-tunneling TEFTs used in this study. Direct bandgap of 0.5 eV $In_{0.88}Ga_{0.12}As$ with work function of 4.7 eV is considered as the low-bandgap semiconductor and direct bandgap of 0.72 eV GaSb with the work function of 4.12 eV is considered as the relatively high-bandgap semiconductor. Table 1 shows the parameters of TFETs used in investigation.

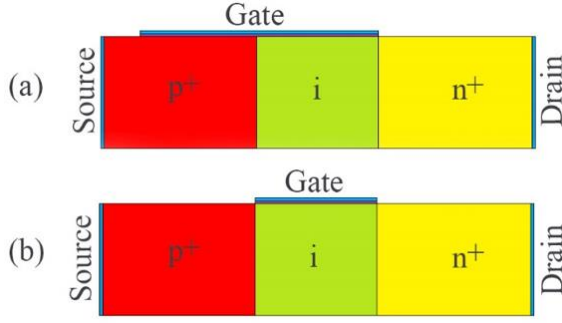The simulations were done using the Silvaco software package and using non-local tunneling.

Figure 1. Schematic structures of (a) line-tunneling and (b) point- tunneling, TFETs

Table 1. Parameters of TFETs

Gate-source overlap length	80 nm
Channel length	50 nm
Body thickness	40 nm
Source doping concentration	8×10^{18} cm^{-3}
Drain doping concentration	10^{18} cm^{-3}
Channel doping concentration	10^{16} cm^{-3}
Gate insulator material	HfO$_2$
Gate insulator thickness	1 nm

2.2 Analytical model

The analytical model used in this paper is line-tunneling TFET analytical model presented in ref. [22] in which the minimum tunnel path is calculated as an indicator of line-tunneling TFETs. In this model minimum tunnel path (l_{min}) and maximum tunnel path (l_{max}), are expressed in Eq. (1) and Eq. (2) as follows

$$l_{max} = \sqrt{2\varepsilon E_g / q^2 N_a} \qquad (1)$$

where, ε is the dielectric permittivity of the semiconductor, E_g is the bandgap energy of the semiconductor, N_a is the source doping concentration and q is the electron charge.

$$l_{min} = l_{max}.(\sqrt{q\psi_s / E_g} - \sqrt{q\psi_s / E_g - 1}) \qquad (2)$$

where, ψ_s is the surface potential at the semiconductor-insulator interface. For small body-effect coefficient (γ), can be written as follows

$$\psi_s = V_{gs} - V_{fb} - \gamma \sqrt{V_{gs} - V_{fb}} \qquad (3)$$

where, V_{fb} is the flat-band voltage. The drain current of the low-bandgap line-tunneling TEFT is written based on l_{min} parameter as follows

$$I = (AqN_a E_g^{1/2} l_{max} / 12\varepsilon).(l_{max} / l_{min})^3 . \exp(-BqE_g^{1/2} L_{min}) \qquad (4)$$

In this paper, the coefficients $A=q^2 \sqrt{m_r} / 18\pi\hbar^2$ and $B=\pi\sqrt{m_r}/2\hbar q$ in Eq. (4), for line-tunneling TFET based on In$_{0.88}$Ga$_{0.12}$As semiconductor are 2.64×10^{20} eV$^{1/2}$.V^{-2}.cm^{-1}.s^{-1} and 15.44×10^6 V.cm^{-1}.eV$^{-3/2}$, respectively. Here m_r and $\hbar$ are the reduced mass and the reduced Plank's constant respectively.

2.3 Operation investigation

The lateral tunneling or point-tunneling occurs in parallel with the semiconductor-gate insulator surface while vertical tunneling happens perpendicular with the semiconductor-gate-insulator surface in the gate-source overlap. Vertical tunneling is also called line-tunneling since the vertical tunneling area is similar to a line which becomes important in higher V_{gs} [23]. Figures 2(a) and 2(b) show the simulated I_{ds}-V_{gs} characteristics of line- and point-tunneling TFETs for In$_{0.88}$Ga$_{0.12}$As and GaSb. It can be seen that the line-tunneling TEFT in both semiconductors has a higher on-current and smaller subthreshold swing than the point-tunneling TFET. To be exact, point subthreshold swings are 8.5 mV/dec and 15.84 mV/dec for In$_{0.88}$Ga$_{0.12}$As line- and point-tunneling TFETs respectively, and 11.84 mV/dec and 32.75 mV/dec for GaSb line- and point-tunneling TFETs respectively.
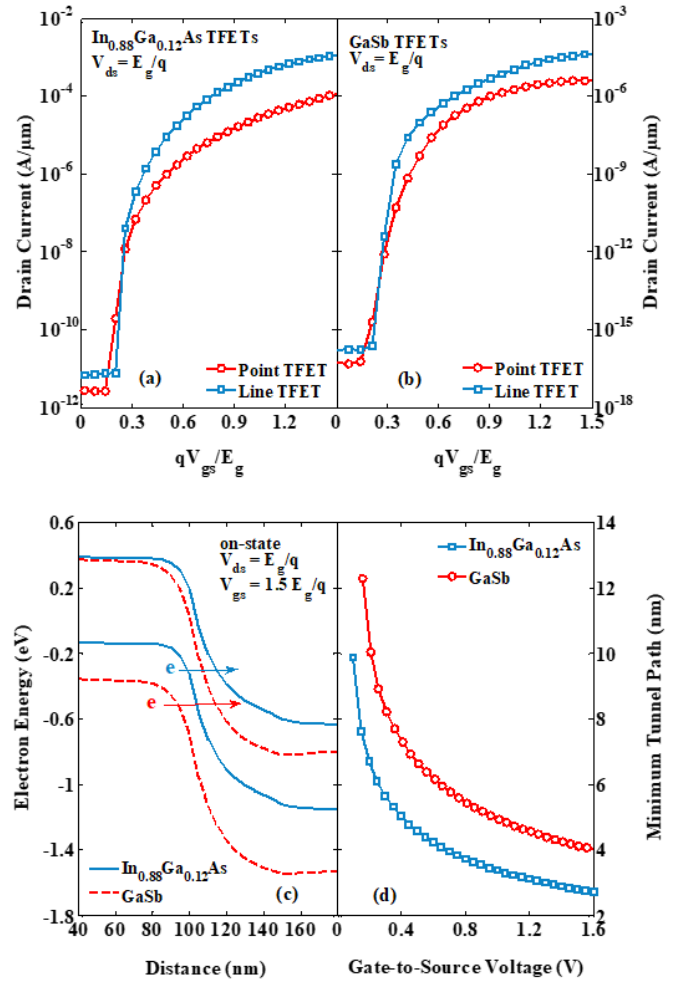

Figure 2. I_{ds}–V_{gs} characteristics for point- and line-tunneling TFETs using (a) In$_{0.88}$Ga$_{0.12}$As, and (b) GaSb. (c) on-state energy-bands diagram of In$_{0.88}$Ga$_{0.12}$As and GaSb line-tunneling TFETs. (d) Calculated on-state minimum tunnel path as function of gate voltage for In$_{0.88}$Ga$_{0.12}$As and Gasb line-tunneling TFETs

In the line-tunneling TFET, as V_{gs} is increasing, charge inversion is formed beneath the gate in the source region and electrons tunnel from the source to the newly inverted source region. When V_{gs} is close to the threshold voltage, this tunneling increases and decreases the subthreshold swing of line-tunneling TFET. Furthermore, in the line-tunneling TFET,

both line-tunneling and point-tunneling are done and there are more electrons in the channel; therefore, on-current of the line-tunneling TFET becomes higher than point-tunneling TFET. Figure 2(a) and 2(b) also show that the line-tunneling TEFT based on $In_{0.88}Ga_{0.12}As$ low-bandgap semiconductor has higher on-current and smaller subthreshold swing than the line-tunneling TFET based on GaSb high-bandgap semiconductor. Figure 2(c) shows the on-state energy-bands diagram of the $In_{0.88}Ga_{0.12}As$ and GaSb TEFTs. As it is seen in these energy-bands diagram, the $In_{0.88}Ga_{0.12}As$ TEFT has a smaller tunnel length than the GaSb high-bandgap TEFT. The smaller tunnel length results in more BTBT generation and consequently increase in the on-current.
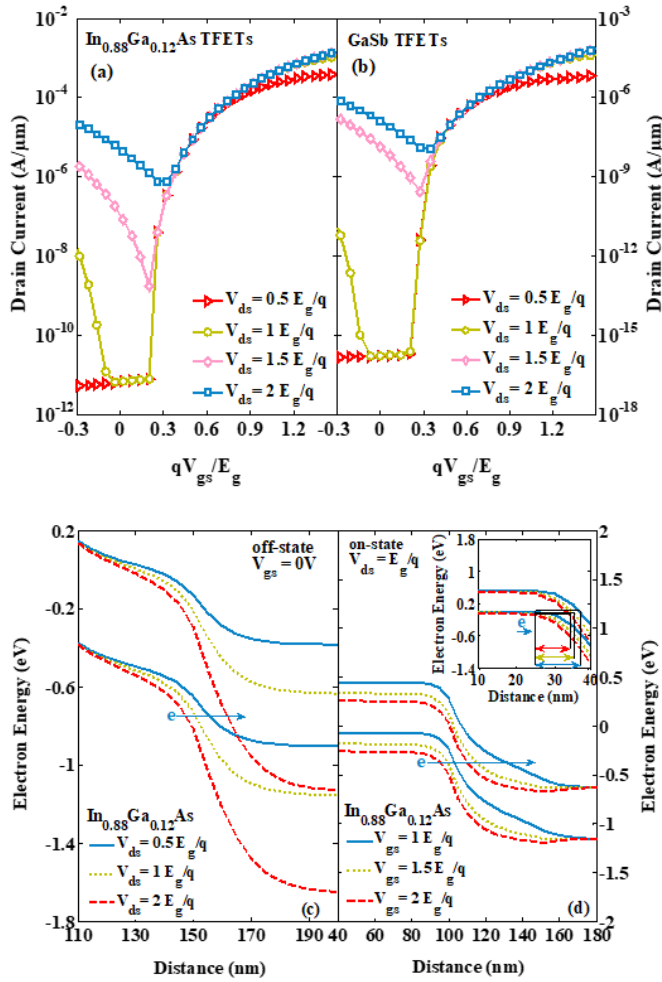

Figure 3. I_{ds}–V_{gs} characteristics for line-tunneling TEFTs using (a) $In_{0.88}Ga_{0.12}As$ and (b) GaSb, for various drain-source voltages. (c) off-state energy-bands diagram of $In_{0.88}Ga_{0.12}As$ line-tunneling TFETs for various drain-source voltages. (d) on-state energy-bands diagram of $In_{0.88}Ga_{0.12}As$ line-tunneling TFETs for various gate-source voltages

Figure 2(d) shows the calculation of l_{min} as function of V_{gs} for two semiconductors $In_{0.88}Ga_{0.12}As$ and GaSb. As it is observed, l_{min} is strongly dependent on E_g. The $In_{0.88}Ga_{0.12}As$ line-tunneling TEFT, has smaller l_{min} than GaSb. This issue causes sooner initiation of line-tunneling that results in the improvement of subthreshold swing and higher on-current of the $In_{0.88}Ga_{0.12}As$ line-tunneling TEFT compared with GaSb line-tunneling TEFT. Figures 3(a) and 3(b) show the dependence of the I_{ds}–V_{gs} characteristic of the simulated line-tunneling TEFTs for different values of V_{ds} for two

semiconductors. As V_{ds} goes higher than bandgap voltage (E_g/q), undesirable tunneling at channel-drain side increases because the tunnel length at the channel-drain side becomes thinner and it also increases off-current and subthreshold swing while, the increase of on-current is negligible. Figure 4(c) shows off-state energy-bands diagram for $In_{0.88}Ga_{0.12}As$ TFET for different values of V_{ds}. In this figure, the narrowing of channel-drain side tunnel length is well seen. Moreover, increase in V_{ds} also increases the diode leakage current and helps increase the off-current. In order to avoid increase in the off-current and also improve the subthreshold swing, V_{ds} for both semiconductors is assumed to be equal to the bandgap voltage (E_g/q) of that semiconductor. Figure 2(d) shows that the variations of l_{min} with V_{gs} are exponential for both semiconductors and this shows the extreme dependence of l_{min} to V_{gs}. The decrease in l_{min} with increase in V_{gs} leads to increase in the on-current and improvement of the subthreshold swing. However, l_{min} is saturated and on-current almost remains stable for high V_{gs}. Figure 3(d) shows the on-state energy-bands diagram of $In_{0.88}Ga_{0.12}As$ line-tunneling TEFT for different values of V_{gs}. Increase in V_{gs} results in a reduction of the tunnel length and it causes an increase in BTBT generation and consequently an increase in the on-current and improvement in the subthreshold swing. However, lowering of tunnel length is saturated and on-current almost remains constant for high V_{gs}. The value of V_{gs} was considered to be 1.5 times that of the bandgap voltage (E_g/q) of that semiconductor in order to assure the high on-current and desirable subthreshold swing.

3. DESIGN OF LOW-BANDGAP LINE-TUNNELING TFET

3.1 Source doping concentration

Figures 4(a) and 4(b) show the dependence of the line-tunneling TEFT current on the source doping concentration for two $In_{0.88}Ga_{0.12}As$ and GaSb semiconductors. As the source concentration increases, the off-current decreases due to increased recombination of the carriers participating in the off-current; In addition, the on-current increases and the subthreshold swing decreases. However, it can be seen that for heavy doping concentrations, the subthreshold swing increases again. The increase in the source doping concentration decreases the point-tunneling onset voltage while it increases the line-tunneling onset voltage and also the on-current of line-tunneling [23]. For high source doping concentrations when V_{gs} becomes near the threshold voltage, vertical tunneling is more effective in determining the subthreshold swing conditions. However, for heavy source doping concentrations, the line-tunneling onset voltage increases and lateral tunneling becomes dominant in determining the subthreshold swing conditions. Using a source with heavy doping concentration provides the considered on- and off-current; but increases the subthreshold swing. Figure 4(c) shows the on-state energy-bands diagram of $In_{0.88}Ga_{0.12}As$ line-tunneling TFET. It can be seen that increasing the source doping concentration causes decrease of the tunnel length that results in an increase in the on-current. However, in heavy doping concentrations the decrease in the tunnel length is saturated and the tunneling generation and consequently the on-current stays approximately constant. Figure 4(d) shows the calculated l_{min} for different values of the source doping concentration for two semiconductors. With increase in the

source doping concentration, l_{min} decreases and becomes saturated in heavy doping concentrations and the on-current stays approximately constant. Thus, the source doping concentration has been considered to 8×10^{18} cm^{-3} in order to improve the conditions of subthreshold swing.
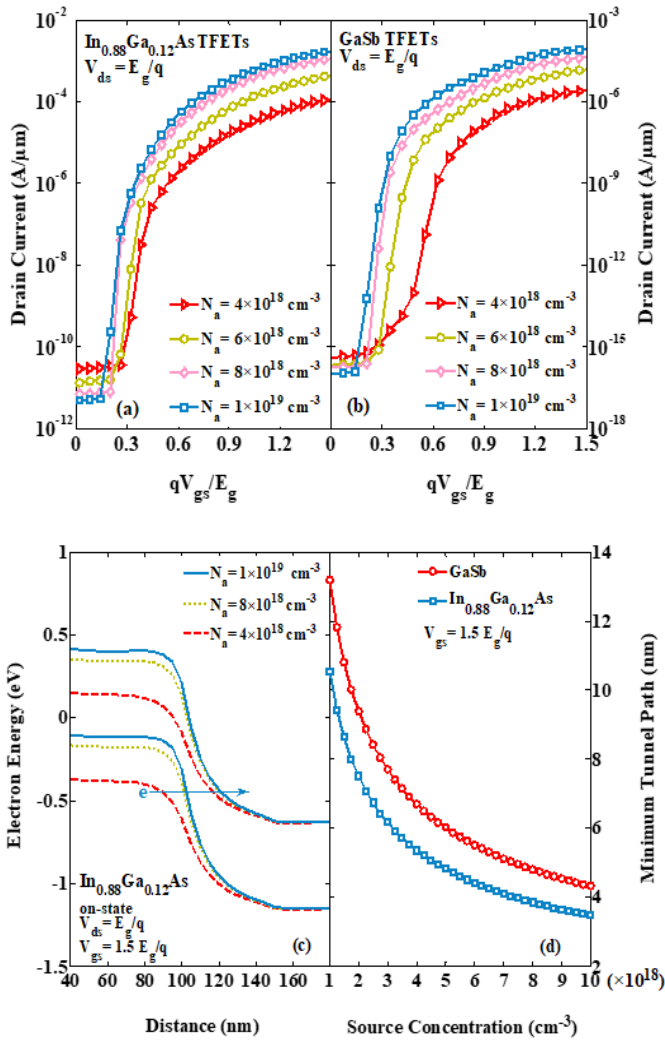

Figure 4. I_{ds}–V_{gs} characteristics for line-tunneling TEFTs using (a) In$_{0.88}$Ga$_{0.12}$As and (b) GaSb, with various source doping concentrations. (c) on-state energy-bands diagram of In$_{0.88}$Ga$_{0.12}$As line-tunneling TFETs for various source doping concentrations. (d) Calculated on-state minimum tunnel path against source doping concentration for In$_{0.88}$Ga$_{0.12}$As and GaSb line-tunneling TFETs

3.2 Gate-insulator material

Figures 5(a) and 5(b) show the I_{ds}-V_{gs} characteristics for three different gate-insulators of Si$_3$N$_4$, Al$_2$O$_3$ and HfO$_2$, for two In$_{0.88}$Ga$_{0.12}$As and GaSb semiconductors. As it can be seen, the gate-insulator material does not affect the off-current but with increasing the dielectric constant, the on-current and the subthreshold swing improve. Figure 5(c) shows the on-state energy-bands diagram of the line-tunneling TEFT for two different gate-insulators of HfO$_2$ and Si$_3$N$_4$. Using the gate-insulator with the higher dielectric constant causes a more powerful capacitor and more bending of energy-bands; thus tunneling begins at a lower voltage and the on-current increases and the subthreshold swing decreases. Calculating the minimum tunnel path in Figure 5(d) shows that using the

gate-insulator with higher dielectric constant decreases the l_{min} in lower V_{gs} and causes the tunneling to begin in a lower voltage. The smaller l_{min} at higher dielectric constants justifies the higher on-current and the lower subthreshold swing of TEFTs.
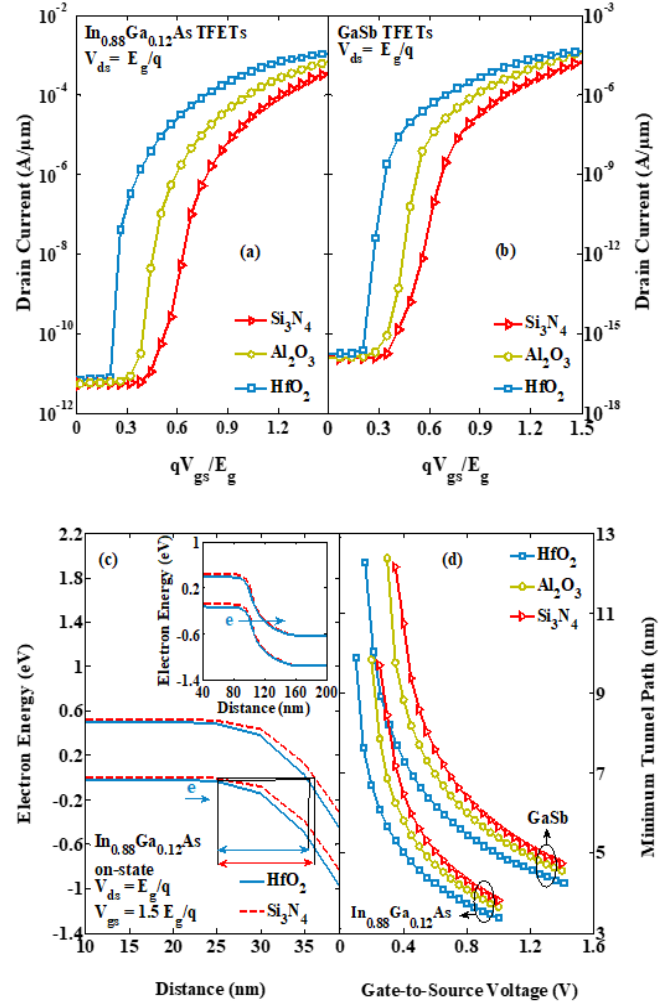

Figure 5. I_{ds}–V_{gs} characteristics for line-tunneling TFETs using (a) In$_{0.88}$Ga$_{0.12}$As, and (b) GaSb, for different gate-insulators. (c) on-state energy-bands diagram of In$_{0.88}$Ga$_{0.12}$As line-tunneling TFETs for two different gate-insulators. (d) Calculated on-state minimum tunnel path as function of gate voltage for In$_{0.88}$Ga$_{0.12}$As and GaSb line-tunneling TFETs for different gate-insulators

3.3 Gate-insulator thickness

Changing the thickness of the gate-insulator does not have much effect on the off-current. However, as it is seen in Figure 6(a) and 6(b) that using a thinner gate-insulator has improved the on-current and the subthreshold swing. Figure 6(c) shows the on-state energy-bands diagram of the In$_{0.88}$Ga$_{0.12}$As line-tunneling TEFT for two different gate-insulator thicknesses. For a thin gate-insulator thickness, the bending of the energy-bands has increased because of the higher gate capacitor. Also, l_{min} increases linearly with the increase in gate-insulator thickness in the calculations done as shown in Figure 6(d). However, the reduction of the gate-insulator thickness is a weak function in reducing the minimum tunnel path; while a thin gate-insulator initiates tunneling at a small V_{gs} and improves the on-current and the subthreshold swing.
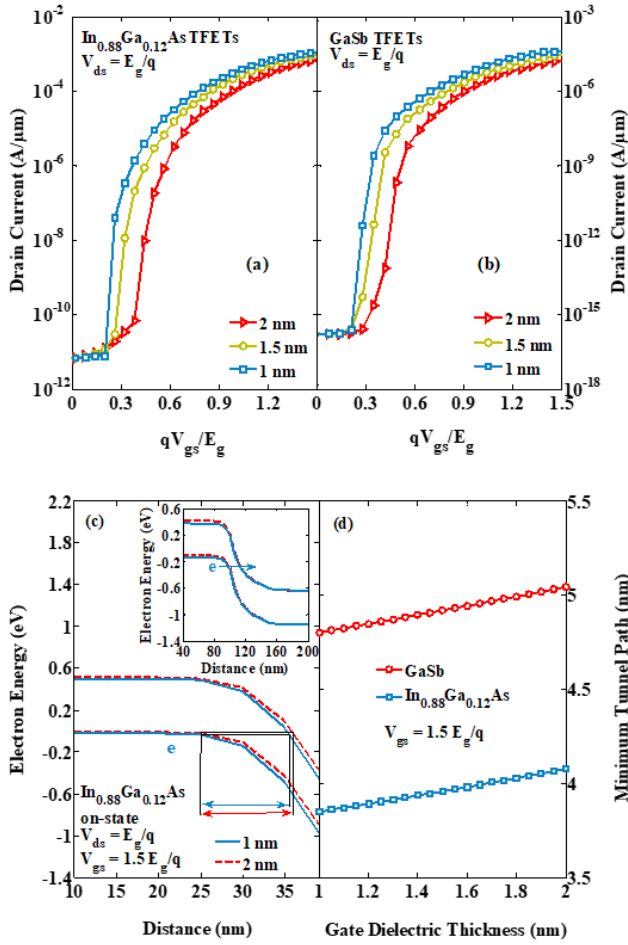
Figure 6. I_{ds}–V_{gs} characteristics for line-tunneling TFETs using (a) $In_{0.88}Ga_{0.12}As$, and (b) GaSb, for various Gate-insulator thicknesses. (c) on-state energy-bands diagram of $In_{0.88}Ga_{0.12}As$ line-tunneling TFETs for various Gate-insulator thicknesses. (d) Calculated on-state minimum tunnel path against Gate-insulator thickness for $In_{0.88}Ga_{0.12}As$ and GaSb line-tunneling TFETs

4. ANALYTICAL DRAIN CURRENT EQUATION FOR LOW-BANDGAP LINE-TUNNELING TFET

Since low-bandgap line-tunneling TFET current of Eq. (4) is complicated, in this section we simplify the current equation for $In_{0.88}Ga_{0.12}As$ low-bandgap semiconductor by appropriate approximations, without losing accuracy. By inserting Eq. (2) in the pre-exponential term $(l_{max}/l_{min})^3$ of Eq. (4) we have the following:

$$(l_{max}/l_{min})^3 = [1/(\sqrt{q\psi_s/E_g} - \sqrt{q\psi_s/E_g - 1})]^3 \quad (5)$$

If we multiply $1/(\sqrt{q\psi_s/E_g} - \sqrt{q\psi_s/E_g - 1})$ in Eq. (5) by $(\sqrt{q\psi_s/E_g} + \sqrt{q\psi_s/E_g - 1})/(\sqrt{q\psi_s/E_g} + \sqrt{q\psi_s/E_g - 1})$, after approximation and simplification we have the following:

$$(l_{max}/l_{min})^3 \cong (2q\psi_s/E_g + 1/9)^2 - 4.16 \quad (6)$$

On the other hand, by inserting Eq. (2) in the exponential term in Eq. (4) and multiplying exponential argument by:

$$(\sqrt{q\psi_s/E_g} + \sqrt{q\psi_s/E_g - 1})/(\sqrt{q\psi_s/E_g} + \sqrt{q\psi_s/E_g - 1}),$$

we have,

$$\exp(-BqE_g^{1/2}l_{min})$$
$$= \exp[-BqE_g^{1/2}l_{max}\sqrt{E_g/q}/(\sqrt{\psi_s} + \sqrt{\psi_s - E_g/q})] \quad (7)$$

Since the fraction term in Eq. (7) is rather complicated, it can be approximated as:

$$\exp(-BqE_g^{1/2}l_{min})$$
$$\cong \exp(-Bq^{1/2}E_g l_{max}/2\sqrt{\psi_s - E_g/2q}) \quad (8)$$

If $k_1 = AqN_aE_g^{1/2}l_{max}/12\varepsilon$ and $k_2 = Bq^{1/2}E_g l_{max}/2$ by inserting Eq. (6) and Eq. (8) in Eq. (4), we have,

$$I \cong k_1[(2q\psi_s/E_g + 1/9)^2 - 4.16]$$
$$.\exp(-k_2/\sqrt{\psi_s - E_g/2q}) \quad (9)$$

By inserting Eq. (3) in Eq. (9), we have,

$$I \cong k_1[(2q(V_{gs} - V_{fb} - \gamma\sqrt{V_{gs} - V_{fb}})/E_g + 1/9)^2 - 4.16]$$
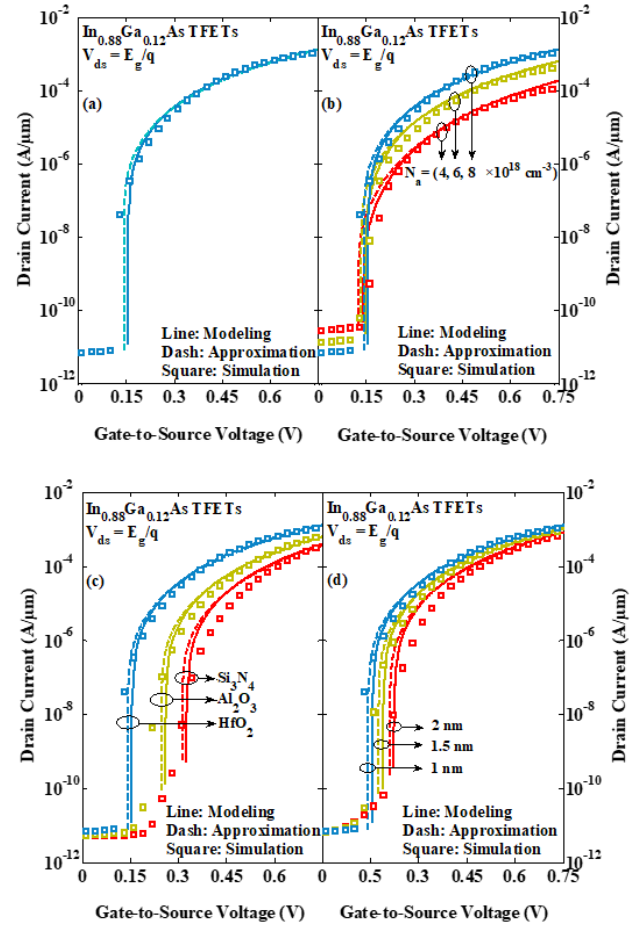$$.\exp[-k_2/(V_{gs} - V_{fb} - \gamma\sqrt{V_{gs} - V_{fb}}) - E_g/2q)^{1/2}] \quad (10)$$

Figure 7. The I_{ds}–V_{gs} characteristics for $In_{0.88}Ga_{0.12}As$ line-tunneling TEFTs of equation (4), and (10) and results of simulation for (a) the main parameters of the paper, (b) three different values of source concentration, (c) three different gate-insulators, and (d) three different thicknesses of gate-insulators

In Figure 7 that shows a comparison between the drain current from Eq. (4) and the drain current from simplified Eq. (10) and the results of drain current obtained from the simulation for various different source doping concentrations and the gate-insulators with different materials and thicknesses indicates a good agreement. This indicates that the approximations made are correct.

5. CONTROLLING THE OFF-CURRENT
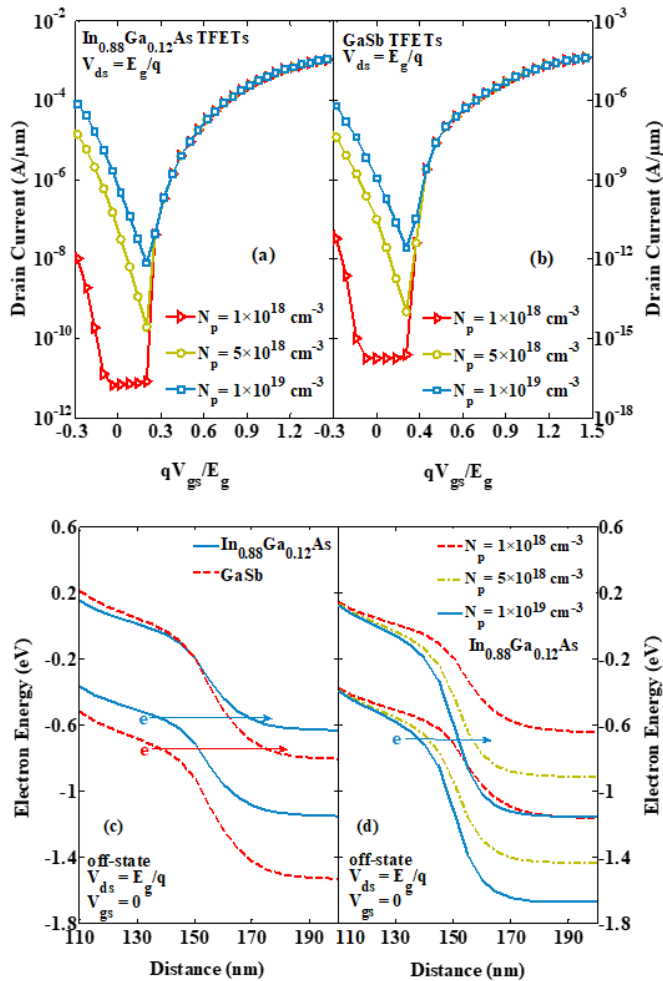
5.1 Drain doping concentration

Figure 8. I_{ds}–V_{gs} characteristics for line-tunneling TEFTs using (a) $In_{0.88}Ga_{0.12}As$ and (b) GaSb, for various drain doping concentrations. (c) off-state energy-bands diagram of $In_{0.88}Ga_{0.12}As$ and GaSb line-tunneling TFETs. (d) off-state energy-bands diagram of $In_{0.88}Ga_{0.12}As$ TFETs for various drain concentrations

The drain doping concentration does not have any effect on the TEFT's on-current. Controlling the drain doping concentration plays an important role in controlling the off-current in TEFTs [16]. Figures 8(a) and 8(b) show the I_{ds}–V_{gs} characteristics of the line-tunneling TEFTs for different values of drain doping concentration for two semiconductors. It can be seen that with increase in the drain doping concentration, the off-current of line-tunneling TEFT and its subthreshold swing have increased while the on-current is fixed. The TEFT energy-bands diagram in the off-state have been drawn for two $In_{0.88}Ga_{0.12}As$ and GaSb semiconductors in Figure 8(c). It can

be seen that in the $In_{0.88}Ga_{0.12}As$ line tunneling TEFT, the tunnel length of the channel-drain side is smaller; that results in the undesirable tunneling of the channel-drain side being more and this issue justifies its higher off-current. Figure 8(d) shows the TEFT energy-bands diagram of $In_{0.88}Ga_{0.12}As$ in the off-state for different amounts of drain concentration. For high doping concentrations, the tunnel length of the channel-drain side decreases that results in an increase in the undesirable tunneling of electrons from the drain side and increases the off-current considerably. Increase in the off-current also increases the subthreshold swing. Using the drain with lower doping concentration decreases the off-current and improves the subthreshold swing. Although we must consider that in very low doping concentrations, a good ohmic connection is not established well on the drain side [3].

6. CONCLUSIONS

It was shown that using the low-bandgap line-tunneling TFET increases the on-current and improves the subthreshold swing. Important design factors such as source doping concentration, the material and thickness of the gate-insulator were considered by simulation and numeral calculations based on the minimum tunnel path. The factor that affects the off-current of the line-tunneling TFET is the drain doping concentration and its effect on the off-current was specified. The drain current equation of low-bandgap line-tunneling TFET was reformulated in a simpler form based on the gate-source voltage and it was shown that simplified equation is an agreement with the proposed drain current equation and simulation results.

REFERENCES

[1] Hu, C. (2008). Green transistor as a solution to the IC power crisis. Proceeding of 9th IEEE International Conference on Solid-State and Integrated-Circuit Technology, Beijing, pp. 16-20. https://doi.org/10.1109/ICSICT.2008.4735116

[2] Ionescu, A.M., Riel, H. (2011). Tunnel field-effect transistors as energy-efficient electronic switches. Nature, 479(7373): 329-337. https://doi.org/10.1038/nature10679

[3] Boucart, K. (2010). Simulation of double-gate silicon tunnel FETs with a high-k gate dielectric (No. THESIS). EPFL. https://doi.org/10.5075/epfl-thesis-4729

[4] Zhao, H., Chen, Y., Wang, Y., Zhou, F., Xue, F., Lee, J. (2011). InGaAs tunneling field-effect-transistors with atomic-layer-deposited gate oxides. IEEE Transactions on Electron Devices, 58(9): 2990-2995. https://doi.org/10.1109/TED.2011.2159385

[5] Choi, W.Y., Park, B.G., Lee, J.D., Liu, T.J.K. (2007). Tunneling field-effect transistors (TFETs) with subthreshold swing (SS) less than 60 mV/dec. IEEE Electron Device Letters, 28(8): 743-745. https://doi.org/10.1109/LED.2007.901273

[6] Koester, S., Lauer, I., Majumdar, A., Cai, J., Sleight, J., Bedell, S., Koswatta, S. (2010). Are Si/SiGe tunneling field-Effect transistors a good idea? ECS Transactions, 33(6): 357-361. https://doi.org/10.1149/1.3487566

[7] Guo, P., Yang, Y., Cheng, Y., Han, G., Pan, J., Ivana, Yeo, Y.C. (2013). Tunneling field-effect transistor with

Ge/In0. 53Ga0. 47As heterostructure as tunneling junction. Journal of Applied Physics, 113(9): 094502. https://doi.org/10.1063/1.4794010

[8] Vandenberghe, W.G., Verhulst, A.S., Groeseneken, G., Soree, B., Magnus, W. (2008). Analytical model for a tunnel field-effect transistor. Melecon 2008. Proceedings of the IEEE 14th Mediterranean Electrotechnical conference. Ajaccio, France, pp. 923-928. https://doi.org/10.1109/MELCON.2008.4618555

[9] Wang, P.F., Hilsenbeck, K., Nirschl, T., Oswald, M., Stepper, C., Weis, M., Hansch, W. (2004). Complementary tunneling transistor for low power application. Solid-State Electronics, 48(12): 2281-2286. https://doi.org/10.1016/j.sse.2004.04.006

[10] Bhuwalka, K.K., Schulze, J., Eisele, I. (2004). Performance enhancement of vertical tunnel field-effect transistor with SiGe in the δp+ layer. Japanese Journal of Applied Physics, 43(7R): 4073. https://doi.org/10.1143/JJAP.43.4073

[11] Seabaugh, A.C., Zhang, Q. (2010). Low-voltage tunnel transistors for beyond CMOS logic. Proceedings of the IEEE, 98(12): 2095-2110. https://doi.org/10.1109/JPROC.2010.2070470

[12] Ghosh, B., Akram, M.W. (2013). Junctionless tunnel field effect transistor. IEEE Electron Device Letters, 34(5): 584-586. https://doi.org/10.1109/LED.2013.2253752

[13] Ionescu, A.M., De Michielis, L., Dagtekin, N., Salvatore, G., Cao, J., Rusu, A., Bartsch, S. (2011). Ultra low power: Emerging devices and their benefits for integrated circuits. IEDM 2011. Proceeding of the IEEE International Electron Devices Meeting, Washington DC, USA, pp. 16.1.1-16.1.4. https://doi.org/10.1109/IEDM.2011.6131563

[14] Nayfeh, O.M., ChlÉirighChleirigh, C.N., Hoyt, J.L., Antoniadis, D.A. (2008). Measurement of enhanced gate-controlled band-to-band tunneling in highly strained silicon-germanium diodes. IEEE Electron Device Letters, 29(5): 468-470. https://doi.org/10.1109/LED.2008.920280

[15] Kao, K.H., Verhulst, A.S., Vandenberghe, W.G., Soree, B., Groeseneken, G., De Meyer, K. (2012). Direct and indirect band-to-band tunneling in germanium-based TFETs. IEEE Transactions on Electron Devices, 59(2): 292-301. https://doi.org/10.1109/TED.2011.2175228

[16] Toh, E.H., Wang, G.H., Samudra, G., Yeo, Y.C. (2008). Device physics and design of germanium tunneling field-effect transistor with source and drain engineering for low power and high performance applications. Journal of Applied Physics, 103(10): 104504. https://doi.org/10.1063/1.2924413

[17] Mayer, F., Le Royer, C., Damlencourt, J.F., Romanjek, K., Andrieu, F., Tabone, C., Deleonibus, S. (2008). Impact of SOI, Si1-xGexOI and GeOI substrates on CMOS compatible tunnel FET performance. IEDM 2008. Proceeding of IEEE International Conference in Electron Devices Meeting. San Francisco, CA, USA, pp. 1-5. https://doi.org/10.1109/IEDM.2008.4796641

[18] Nayfeh, O.M., Hoyt, J.L., Antoniadis, D.A. (2009). Strained-Si1-xGex/Si band-to-band tunneling transistors: Impact of tunnel-junction germanium composition and doping concentration on switching behavior. IEEE Transactions on Electron Devices, 56(10): 2264-2269. https://doi.org/10.1109/TED.2009.2028055

[19] Shih, C.H., Chien, N.D. (2011). Sub-10-nm tunnel field-effect transistor with graded Si/Ge heterojunction. IEEE Electron Device Letters, 32(11): 1498-1500. https://doi.org/10.1109/LED.2011.2164512

[20] Toh, E.H., Wang, G.H., Chan, L., Sylvester, D., Heng, C.H., Samudra, G.S., Yeo, Y.C. (2008). Device design and scalability of a double-gate tunneling field-effect transistor with silicon–germanium source. Japanese Journal of Applied Physics, 47(4S): 2593. https://doi.org/10.1143/JJAP.47.2593

[21] Kim, S.H. (2012). Germanium-source tunnel field effect transistors for ultra-low power digital logic. Ph.D. dissertation. University of California, Berkeley, USA.

[22] Shih, C.H., Chien, N.D. (2014). Design and modeling of line-tunneling field-effect transistors using low-bandgap semiconductors. IEEE Transactions on Electron Devices, 61(6): 1907-1913. https://doi.org/10.1109/TED.2014.2316217

[23] Vandenberghe, W.G., Verhulst, A.S., Groeseneken, G., Soree, B., Magnus, W. (2008). Analytical model for point and line tunneling in a tunnel field-effect transistor. 2008 International Conference on Simulation of Semiconductor Processes and Devices, Hakone, Japan, pp. 137-140. https://doi.org/10.1109/SISPAD.2008.4648256

NOMENCLATURE

A	Parameter of Kane's model, $eV^{1/2}.V^{-2}.cm^{-1}.s^{-1}$
B	Parameter of Kane's model, $V.cm^{-1}.eV^{-3/2}$
E_g	Bandgap energy of the semiconductor, eV
$\hbar$	Reduced Plank's constant, eV.s
I_{off}	Off current of TFET, A/µm or A
I_{on}	On current of TFET, A/µm or A
l_{max}	Maximum tunnel path, m
l_{min}	Minimum tunnel path, m
m_r	Reduced mass, Kg
N_a	Source doping concentration, cm^{-3}
N_p	Drain doping concentration, cm^{-3}
q	Electron charge, C
V_{ds}	Drain-to-source voltage, V
V_{fb}	Flat-band voltage, V
V_{gs}	Gate-to-source voltage, V

Greek symbols

γ	Body-effect coefficient, $\sqrt{V}$
ε	Dielectric permittivity of materials
ψ_s	surface potential at the semiconductor-insulator interface, V